WATER ABSORPTION AND EFFECT OF WATER CONTENT ON VISCOSITY AND ELECTRICAL CONDUCTIVITY OF TWO DIETHYLMETHYLAMMONIUM IONIC LIQUIDS

M. Villanueva, C. Fernández-Leira, J. J. Parajó*, Lois Fernández-Míguez, J. Salgado

NaFoMat Group. Applied Physic and Particle Physics Departments. University of Santiago de Compostela.

Campus Vida. 15782 Santiago. Spain

*e-mail: juanjose.parajo@usc.es

Abstract

Since the effect of environmental water on certain properties of Ionic Liquids (ILs) can be decisive when considering a possible industrial application, the effect of environmental water absorption on electrical conductivity (using a conductimeter Crison Basic 30) and viscosity (using a rheometer AR2000 TA Instruments) of two diethylmethylammonium ionic liquids was analyzed. The studied compounds are based on a cation (diethylmethylammonium) and two anions (methanesulfonate and trifluoromethanesulfonate).

In both ionic liquids the water absorption corresponded to a fickian behavior, agreeing with previous literature data of other ILs, being the methanesulfonate much more hygroscopic than the trifluoromethanesulfonate (28% and 6% in weight for [EEMAm][MeSO$_3$] and [EEMAm][OTf], respectively). As it was expected, water considerably increases the ionic conductivity; values were duplicated in case of [EEMAm][OTf] and quadruplicated for [EEMAm][MeSO$_3$]. Likewise, the viscosity decreases drastically with water incorporation in the IL; changes of 88 % and 66% for trifluoromethanesulfonate and methanesulfonate, respectively, were measured.

Furthermore, in the case of diethylmethylammonium trifluoromethanesulfonate, the functional dependence of the viscosity with the molar fraction of water was studied. According to the observed behavior, the viscosity of the pure IL was estimated using the equation proposed by Seddon *et al*.

Keywords: viscosity, ionic conductivity, water absorption.
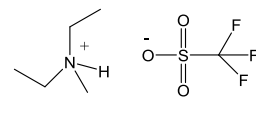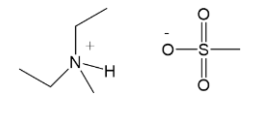
1. Introduction

The study of the environmental water absorption of ionic liquids can modify noticeably its physical properties which can be a problem for specific applications. For example, it could be expected that viscosity vary in a sensitive way in case of the incorporation of environmental water, what would affect seriously to its quality as lubricants. For this and other several reasons, the water absorption of two diethylmethylammonium ionic liquids was analysed. Water absorption by a gravimetric method was studied, until the saturation level of water absorbed was reached. Also, the effect of the saturating water on the ionic liquid range was analysed as well as the variation of the viscosity with water content.

2. Materials and methods

2.1. Chemicals

Main characteristics of the two selected Ionic Liquids (ILs), both supplied by IoLiTec, are indicated in Table I.

Table I. Chemical structure, identification number, molecular mass and purity of the two selected ILs.

Name	Abbreviation CAS number	Chemical structure	Molecular mass	Mass fraction Purity
Diethylmethylammonium trifluoromethanesulfonate	[EEMAm][OTf] 945715-39-9		237.24	>0.98
Diethylmethylammonium methanesulfonate	[EEMAm][MeSO₃] 945715-44-6		183.27	>0.98

2.2. Experimental section
2.2.1. Water absorption measurements

To carry out this study, samples of both liquids in their commercial form (with initial water content of 2.5% in the case of [EEMAm][MeSO$_3$] and 0.3% in the [EEMAm][OTf]), contained in two beakers, were exposed to the laboratory environment during a total period of 67 days, taking regularly data from their mass through a precision scale. It was assumed that the totality of the observed mass variation would correspond to the absorption of water, despising the influence of other possible effects. The absorption process was produced at an ambient temperature between 18 and 20 ºC and with a relative air humidity of around 50%.

2.2.2.Thermal studies
DSC measurements

A differential scanning calorimeter DSC Q100 TA-Instruments was used to determine the different state transitions experimented by the IL during heating and cooling cycles. Liquid nitrogen was used as coolant fluid. The employed methodology and procedure were the same described in previous papers [1].

Measurements for melting and crystallization temperatures were determined as the onset temperature of the corresponding peaks, whereas glass transition was determined to be the midpoint of a heat capacity change.

TGA measurements

A thermogravimetric analyzer (TGA 7-Perkin Elmer) operating in dynamic modes under dry air atmosphere was used to perform thermogravimetric analysis following the methodology and procedure indicated in previous publications [2, 3].

2.2.3. Rheology

The dynamic viscosity of the two ILs was measured at 15 °C under air atmosphere using a TA Instruments AR2000 stress control, with a Peltier cooling device that assures a constant temperature value. Geometry of cone and plate with a diameter of 40 mm, an angle of 1° and a truncation of 30 µm was employed. Both the sample and the geometry were covered with a lid to avoid the exchange of atmospheric water with the environment. Flow curves were obtained with stress-ramped mode

experiments with stress values ranging from 0: 033 to 150 Pa during 10 min. Each essay was repeated at least three times, to ensure the repetition of the technique used.

2.2.4. Conductivity measurements

Electrical conductivity was measured using a conductimeter Crison Basic 30 at temperature of 20 °C. Previous to the conductivity determination, calibration was made with a standard of 1430 µS/cm. Experimental procedure has been done following the indicated in the bibliography [4].

3. Results and discussion

3.1. Water absorption measurements

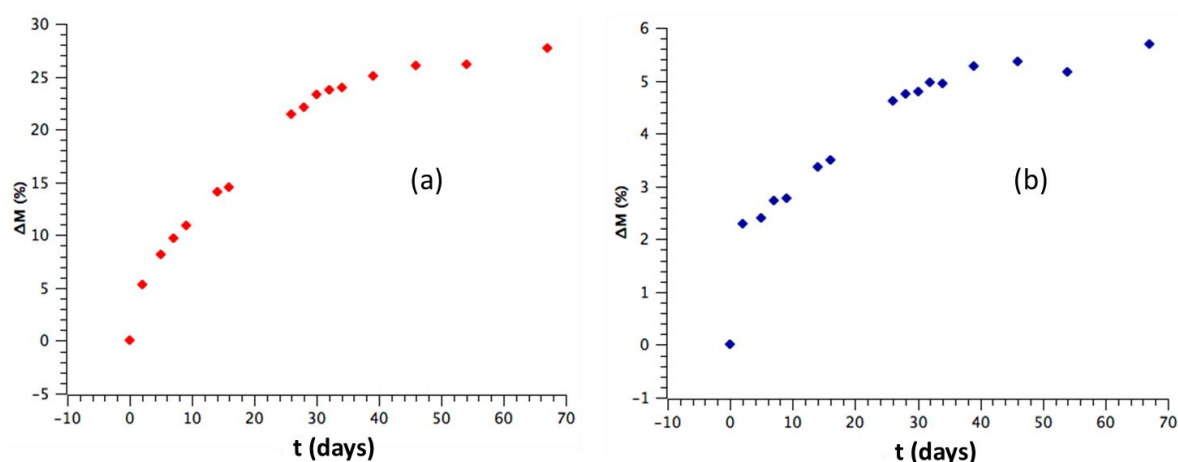Figure 1 shows the mass increases (in %) versus the exposition time for both ionic liquids, [EEMAm][OTf] (a) and [EEMAm][MeSO$_3$] (b).

Figure 1. Water atmospheric absorption curves obtained for the [EEMAm][MeSO$_3$] (a) and [EEMAm][OTf] (b) ILs.

As it can be observed, in both cases a Fickian behavior was observed, with a linear increase at the beginning of the exposition followed by a levelling of the water absorbed reaching a constant value. This tendency was also observed previously by other authors for other ILs [5]. Although, the saturation levels were quite different; in case of [EEMAm][OTf] an increase of 6% in mass was reached, being almost the 28% for [EEMAm][MeSO$_3$], that means the Diethylmethylammonium IL with the methanesulfonate anion much more hygroscopic than that with the trifluoromethanesulfonate one.

3.2. Thermal studies
DSC measurements

In order to study the water effect on the liquid range of these two ILs, DSC and TGA measurements were done. The lower limit of this liquid window has been characterized through solid-liquid transitions and the upper limit was determined using thermogravimetric analysis.

From DSC traces, thermal transitions were characterized through the onset of the corresponding peak (in case of melting and crystallization peaks) or as the midpoint of the heat capacity change in case of the detection of a glass transition. Figure 2 shows the DSC curves corresponding to the last cooling and heating of the ILs samples.
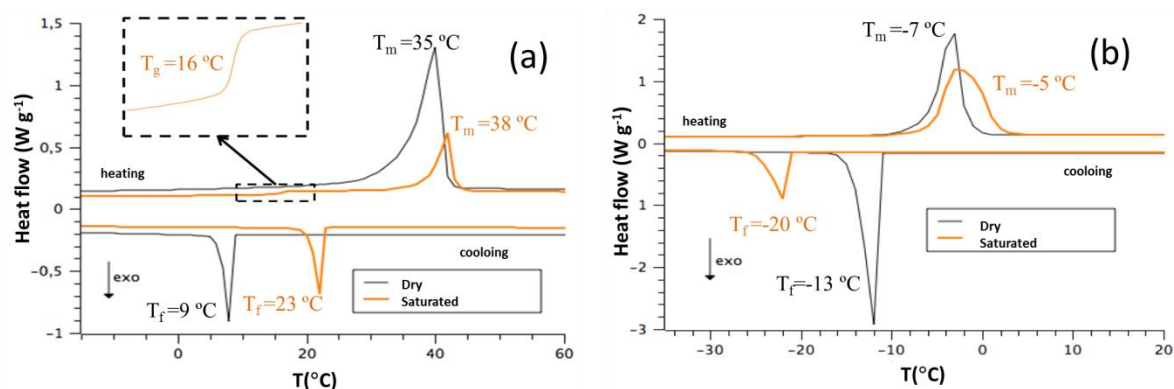
Figure 2. DSC curves obtained for the [EEMAm][MeSO3] (a) and [EEMAm][OTf] (b) dried and saturated samples.

In both liquids it is observed that melting is not affected by water, while freezing change with the presence of water. This is due to the fact that previously to the cooling of the IL corresponding to the figure 2, the IL was subjected to a heating up to 125 ° C for 50 min during which almost all the absorbed water has been released and only a small part may have remained in the sample, affecting to the crystallization phenomenon. Therefore, the peak associated with this last phenomenon does move significantly with respect to the IL without water, in one case towards higher temperatures ([EEMAm][MeSO3]) and in the other towards lower temperatures ([EEMAm][OTf]). In case of [EEMAm][MeSO3] a glass transition was also detected. A possible explanation of this phenomenon could be that the high level of absorbed water may change the structure generating crystalline and also amorphous phases being this last one the responsible of the glass transition detected in the DSC experiments.

TGA measurements

TGA curves obtained for the dried and saturated ILs samples are shown in Figure 3. All experiments were performed at 10 °C · min^{-1}. A first observation is that in saturated samples it was detected a loss mass step almost at the beginning of the experiment that is due to the presence of water. It can be seen that the step change in mass magnitude is very similar to the saturation level of water for the [EEMAm][OTf]. In case of [EEMAm][MeSO3] the whole contain of water does not corresponds to the mass change observed in the first step of the curve, maybe because the heating rate is much high to allows the complete water release, which is still releasing at temperatures higher than 130 °C and that is related to the smooth change in loss mass detected during the second step, overlapped to the degradation of the ionic liquid.
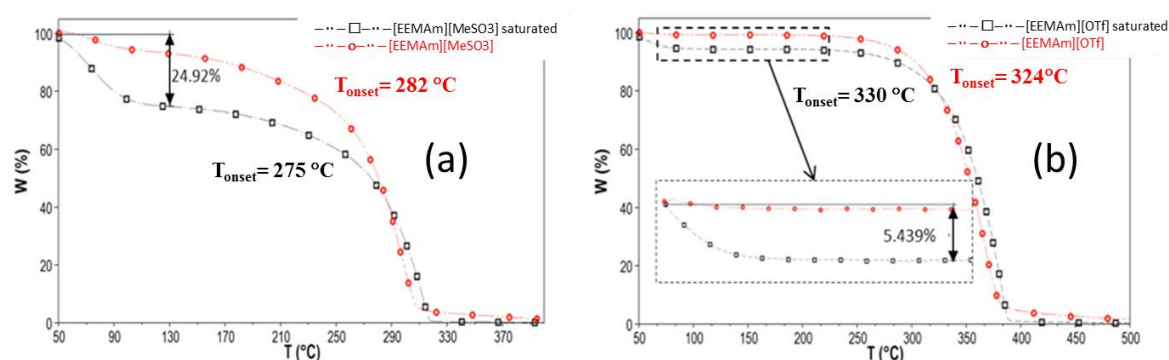

Figure 3. TGA curves obtained at 10 °C · min^{-1} under air atmosphere, for the [EEMAm][MeSO3] (a) and [EEMAm][OTf] (b) dried and saturated samples

Taking into account that the liquid range can be estimated as the difference between onset melting temperature and onset degradation temperature, it can be concluded that the presence of water has no effect on the liquid range, as it observed in Table II.

Table II. Onset temperatures (all in °C) associated to the melting transition (t_m) (DSC) and to the thermal stability (t_d) (TGA) for the two selected ILs.

	Dry			Saturated		
Name	t_m	t_d	Liquid Range	t_m	t_d	Liquid Range
[EEMAm][MeSO₃]	35	282	247	38	275	237
[EEMAm][OTf]	-7	324	331	-5	330	335

$U(t_m)=1°C$, $U(t_d)=5°C$

3.3. Rheology

From the linear part of the flow curves the Newtonian fluid model was applied:

$$\sigma = \eta \cdot \dot{\gamma}$$

Fitting experimental values the above equation, dynamic viscosity values were calculated. Table III shows viscosity values corresponding to the ILs as supplied (η_{supp}) and water saturated (η_{sat})

Table III. Obtained viscosity values corresponding to the two selected ILs "as supplied" and at the saturation level.

	η_{supp} / Pa·s	η_{sat} / Pa·s	-Δη (%)
[EEMAm][MeSO₃]	0.12579 ± 0.00003	0.01463 ± 0.00001	88.37
[EEMAm][OTf]	0.05430 ± 0.00002	0.01872 ± 0.00003	65.53

In order to obtain more information about the influence of the water on the rheological properties of the ILs, a study of the viscosity depending on the water molar fraction in the [EEMAm][OTf] was done.
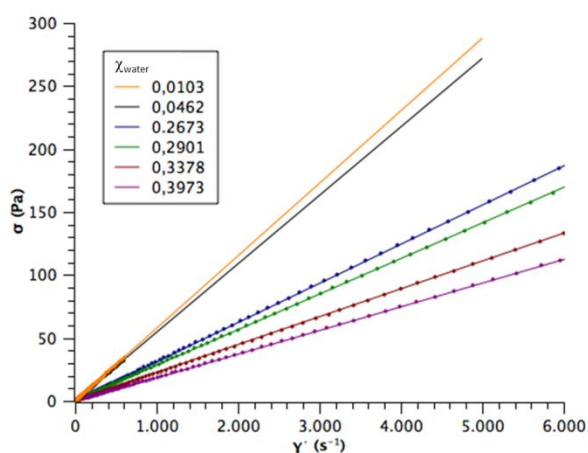

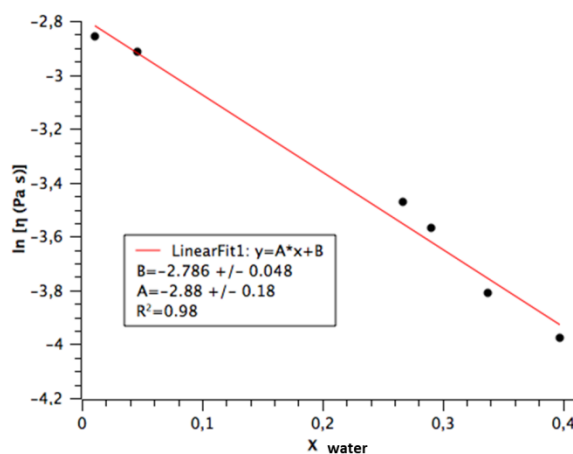Figure 4. Newtonian region for [EEMAm][OTf] with different water contents.

Figure 5. Fitting of experimental values to the equation proposed by Seddon *et al* [6]

In Figure 4, flow curves corresponding to the IL [EEMAm][OTf] with different water contents are presented.

From linear fittings to the Newtonian fluid model, dynamic viscosity values were obtained for each molar fraction, which are indicated in Table IV.

Table IV. Viscosities, molar fractions and decrease of viscosity calculated respect to the degasified sample of [EEMAm][OTf] at 15 °C.

Time (days)	χ_{water}	η (Pa·s)	$\Delta\eta$ (%)
0 (*)	0.01033 ± 0.00004	0.05753 ± 0.00001	-
0	0.04615 ± 0.00004	0.05430 ± 0.00002	5.5993 ± 0.0003
3	0.26726 ± 0.00003	0.03110 ± 0.00001	45.9331 ± 0.0002
5	0.29008 ± 0.00003	0.02819 ± 0.00001	50.9883 ± 0.0002
13	0.33780 ± 0.00003	0.02217 ± 0.00004	61.4568 ± 0.0007
26	0.39734 ± 0.00002	0.01872 ± 0.00003	67.4628 ± 0.0006

(*) degasified sample

As it was expected, a noticeable decrease on the viscosity values is observed as the water content increases. Following the proposition of Seddon *et al.* [6] a plot of $\ln\eta$ versus the molar fraction was depicted, which is presented in Figure 5. Fitting these values to the equation:

$$\eta = \eta_s exp\left[-\frac{\chi_{water}}{a}\right]$$

where η_s is the viscosity of the pure IL.

From Figure 5 it can be seen that the correlation of the experimental data with the above equation is good. The obtained value for the viscosity for the pure IL was 0.0617±0.00390 Pa·s.

3.4. Electrical conductivity

Finally, the electrical conductivity corresponding to the initial samples ("as supplied") and to the saturated ones was measured with a Crison Basic 30 conductimeter. Obtained values at 20 ° C as well as increasing in conductivity (in %) are presented in table V. As it can be seen, an increase of the conductivity with the water is detected as it was expected.

Table V.

σ (mS·cm^{-1})*	As supplied	Saturated	$\Delta\sigma$ (%)
[EEMAm][MeSO$_3$]	4.64	18.00	287.9
[EEMAm][OTf]	7.30	13.02	78.3

* All σ measures were done with a resolution of 1%.

4. Conclusions

In this work the effect of water on different properties of two ionic liquids, [EEMAm][MeSO3] and [EEMAm][OTf] was studied, being the following the main conclusions:

- No noticeable effects on the liquid range of both ILs were observed, although some change on the morphology of the [EEMAm][MeSO3] can be suspected because of the detection of a glass transition by DSC; in particular the appearance of micro amorphous phases inside the crystalline one.

- A decrease of the viscosity has been detected with the water content. An estimation of the pure [EEMAm][OTf] ionic liquid was done by using the equation proposed by Seddon.

- Determination of the ionic conductivity for the supplied and saturated two selected ionic liquids was done, observing that this physical property decreases with the presence of water at the saturated value.

Conflicts of Interest

The authors declare no conflict of interest.

References

1. M. Villanueva, M.; Parajó,J.J.; Sánchez, P.B.; García, J.; Salgado, J. Liquid range temperature of ionic liquids as potential working fluids for absorption heat pumps. *J. Chem. Thermodyn*. **2015**, 91, 127–135. doi:10.1016/j.jct.2015.07.034.
2. Parajó, J.J.; Villanueva, M.; Otero, I.; Fernández, J.; Salgado J. Thermal stability of aprotic ionic liquids as potential lubricants. Comparison with synthetic oil bases. *J. Chem. Thermodyn*. **2018**, 116, 185–196. doi:https://doi.org/10.1016/j.jct.2017.09.010.
3. Salgado, J.; Parajó, J.J.; Fernández, J.; Villanueva, M. Long-term thermal stability of some 1-butyl-1-methylpyrrolidinium ionic liquids. *J. Chem. Thermodyn*. **2014**, 74, 51–57. doi: https://doi.org/10.1016/j.jct.2014.03.030.
4. Prego, M.; Rilo, E.; Carballo, E; Franjo, C.; Jiménez, E.; Cabeza, O. Electrical conductivity data of alkanols from 273 to 333 K. *J. Mol. Liquids* **2003**, 102, 83–91. https://doi.org/10.1016/S0167-7322(02)00049-1.
5. Cuadrado-Prado, S.; Domínguez-Pérez, M.; Rilo, E.; García-Garabal, S.; Segade, L., Franjo, C.; Cabeza, O. Experimental measurement of the hygroscopic grade on eight imidazolium based ionic liquids *Fluid Phase Equilibria,* **2009**, 278, 36-40. doi:10.1016/j.fluid.2008.12.008.
6. Seddon, K. R.; Stark, A.; Torres, M.J**.** Influence of chloride, water, and organic solvents on the physical properties of ionic liquids *Pure Appl. Chem.*, **2000**, 72(12), 2275-2287